Impact of deep-water renewal events on fixed nitrogen loss from seasonally-anoxic Saanich Inlet

Cara C. Manning, Roberta C. Hamme, & Annie Bourbonnais

2010

https://doi.org/10.1016/j.marchem.2010.08.002

Impact of deep-water renewal events on fixed nitrogen loss from seasonally-anoxic Saanich Inlet

Cara C. Manning*, Roberta C. Hamme, Annie Bourbonnais

School of Earth and Ocean Sciences, University of Victoria, Victoria, BC V8W 3P6, Canada

Abstract

We interpreted profiles of N_2/Ar ratios, δ^{15}N-N_2, and O_2 concentration collected in Saanich Inlet, British Columbia, Canada over an annual cycle. Our measurements and data from a regional cabled observatory indicated that four deep- or bottom-water renewal events occurred over our study period. Each event was correlated with a period of weak tidal currents, such that very low tidal mixing allowed inflowing water to retain its high density as it moved across the sill and into the deeper basin. By quantifying the concentration of excess N_2 in each month and the vertical diffusion rate, we determined that the N_2 production rate ranged from 1.7 $\pm$ 0.3 mmol N_2 m^{-2} d^{-1} in summer to 8.1 $\pm$ 2.8 mmol N_2 m^{-2} d^{-1} in winter. This depth-integrated estimate accounts for all pathways resulting in fixed (bioavailable) nitrogen loss as N_2 gas, including denitrification and anammox, and incorporates any benthic production of N_2 that diffuses into the overlying water column. In spring and summer, the maximum N_2 excess corresponded to the maximum δ^{15}N-N_2, indicating that denitrification approached completion.

*Corresponding author.
Email address: cmanning@alumni.uvic.ca (Cara C. Manning)

In these months, the average isotopic composition of the fixed N consumed was 7.5 ± 1.2‰. Following bottom-water renewal in fall, which brought in nutrient-rich, low-N_2 water, the N_2 concentration increased and became progressively more enriched in ^{15}N. The high rates of N_2 production in Saanich Inlet likely exist in other anoxic basins that undergo periodic deep-water renewal by nitrate-rich waters.

Key words: Anoxic basin, nitrogen cycle, nitrogen isotopes, denitrification, anammox, dissolved oxygen, renewal, monitoring systems, Canada, British Columbia, Saanich Inlet

---

1. Introduction

We present a one-year time series of dissolved oxygen (O_2) concentrations, nitrogen/argon (N_2/Ar) ratios, and isotopic composition of N_2 in Saanich Inlet, British Columbia, Canada. We use these observations to estimate the loss of nutrients from the system by denitrification and related processes. We combine our measurements with data from a regional cabled sea-floor observatory to determine the timing of deep-water renewal and the mechanism for these events. Although this inlet is a small basin of limited global importance by itself, it serves as a model system for fjords with restricted circulation, common in similar geologic settings around the world.

Saanich Inlet, on southeastern Vancouver Island, transitions from sulfidic to oxic deep waters nearly every year and is one of the best-studied anoxic fjords in the world (Tunnicliffe et al., 2003). A 75-m depth sill at the northern end of the inlet restricts exchange into the basin, which reaches a maximum depth of 225 m (Fig. 1). High rates of surface productivity lead to high rates

of aerobic respiration, consuming O_2 in the normally stagnant deep waters (Timothy and Soon, 2001; Gargett et al., 2003). Once O_2 is depleted, bacteria utilize other oxidants such as NO_3^- and SO_4^{2-} to decompose organic matter, typically resulting in complete consumption of NO_3^- and the production of H_2S in the bottom waters by summer (Anderson and Devol, 1973; Emerson et al., 1979). The anoxic basin is usually reoxygenated in early fall when upwelling off the coast of Vancouver Island causes dense water to form outside Saanich Inlet and flow across the sill into the basin (Anderson and Devol, 1973).

In oxygen-deficient environments, microbially-mediated reactions consume bioavailable inorganic nitrogen (fixed N), including nitrate, nitrite and ammonium (NO_3^-, NO_2^- and NH_4^+). These reactions produce N_2 gas and are the dominant mechanism for the loss of fixed N from the ocean (e.g., Hulth et al., 2005). Determining the magnitude of the marine fixed N sink is relevant to the global carbon cycle because the availability of fixed N limits primary production in most of the ocean (Smith, 1984; Tyrrell, 1999). Over the past decade, new measurements have fuelled debate over whether the fixed N budget is balanced in the modern ocean (Gruber, 2004; Codispoti, 2007). In particular, the rate of fixed N loss outside of the ocean's major oxygen minimum zones is crudely quantified, but globally significant (Codispoti, 2007). The coastal fixed N sink may be increasing as eutrophication expands the extent of intermittently and permanently anoxic waters and sediments (Larsson et al., 1985; Malakoff, 1998; Naqvi et al., 2000). The regular ventilation of Saanich Inlet makes it an ideal location to investigate the effects of deep-water renewal on fixed N loss as a model for other intermittently anoxic

zones.

Until recently, the dominant process contributing to marine fixed N loss was thought to be denitrification, the sequential reduction of NO_3^- to N_2 and simultaneous oxidation of another compound such as organic matter (Devol, 2003). However, numerous studies have now confirmed the presence of anammox bacteria that use NO_2^- to anaerobically oxidize NH_4^+ to N_2 and have demonstrated that anammox dominates fixed N loss in some environments (Dalsgaard et al., 2003; Kuypers et al., 2003, 2005; Thamdrup et al., 2006). Quantifying fixed N loss from the N_2 excess is a relatively new method, reported for only two marine oxygen-deficient zones to date: the Arabian Sea (Devol et al., 2006) and the Black Sea (Fuchsman et al., 2008). This method requires no assumptions about the form of fixed N consumed, nor the process responsible. The N_2 excess we measure is derived from natural conditions in seawater and integrates over larger spatial and temporal scales than bottle incubations or benthic enclosures (Groffman et al., 2006), but cannot provide instantaneous rates. Our method estimates water column N_2 production, along with any N_2 produced in the sediments that diffuses into the water column.

Mixing with adjacent oxygenated water impacts all anoxic zones, both by bringing new fixed N into the region and by redistributing chemicals within the basin. However, the timing, mechanisms, and ecological impacts of intrusion events are often poorly understood due to insufficient sampling (Berelson, 1991; Glazer et al., 2006; Pawlowicz et al., 2007a). Hannig et al. (2007) demonstrated that the dominant pathway to fixed N loss changed from denitrification to anammox over several years in response to an inflow

event in the Gotland Deep, and Fuchsman et al. (2008) hypothesized that the extent of and pathways to fixed N loss may vary with time in the Black Sea. With a time series of measurements, we characterize the effects of multiple inflow events on fixed N loss rates at our location.

2. Methods

2.1. Study site and sampling apparatus

We collected ten CTD profiles at 48° 39' N, 123° 30' W (Fig. 1), close to the inlet mouth, between April 2008 and April 2009 using a SeaBird instrument with dissolved O_2 and photosynthetically active radiation (PAR) sensors. The station has a maximum depth of ∼190 m, while the sill is at 75 m. Discrete samples for measurements of N_2/Ar ratios, δ^{15}N-N_2, and dissolved O_2 concentration were collected in duplicate on nine of these cruises. In April 2009, we collected a profile of these measurements outside of Saanich Inlet in Haro Strait (347 m depth, 48° 41' N, 123° 15' W), where water column fixed N loss does not occur. Gas samples were collected from 2-L Niskin bottles. A bucket with a spigot was used to collect surface samples starting in June 2008, in order to capture the extremely shallow mixed layer (often <1 m depth). Nutrient concentrations and the isotopic compositions of NO_3^- and NH_4^+ were measured by A. Bourbonnais for all dates where gas samples were collected and will be presented in a future publication.

2.2. Measurement of N_2/Ar ratios, δ^{15}N-N_2, and O_2 concentration

Dissolved O_2/N_2/Ar ratio and δ^{15}N-N_2 measurements were made following Emerson et al. (1999). Evacuated 185-mL glass flasks containing dried

$HgCl_2$ were filled halfway with seawater, using tubing flushed with CO_2 to prevent air contamination. Flasks featured Louwers-Hapert valves with two sealing O-rings, and a vacuum was kept between the two O-rings before and after sampling (Hamme and Emerson, 2004b). After weighing, the water was equilibrated with the headspace and then removed.

The headspace gas was purified with a liquid N_2 trap, for complete removal of CO_2 and water vapor, and then analyzed on a stable isotope ratio mass spectrometer (IRMS). Isotope measurements are referenced to local air and corrected for isotopic fractionation between the water and headspace in the flasks (Knox et al., 1992). The precisions of N_2/Ar ratios and δ^{15}N-N_2 averaged $\pm 0.06\%$ and $\pm 0.01‰$, respectively, both based on duplicates.

Carbon monoxide in the IRMS ion source can positively bias δ^{15}N-N_2 measurements because CO has the same mass as N_2, but ^{13}C:^{12}C ratios are naturally higher than ^{15}N:^{14}N ratios. Removal of sample CO_2 by liquid N_2 eliminates this effect for most samples by preventing CO generation in the source (Bender et al., 1994), but does not remove CO naturally present in the sample. Carbon monoxide is photochemically produced in surface waters (Conrad and Seiler, 1980; Jones, 1991) and therefore may affect our δ^{15}N-N_2 measurements in the euphotic zone (upper 15 m on average, based on the depth of 1% surface incident irradiance from the PAR sensor). However, CO interference should not affect deeper samples, because CO is rapidly consumed at depth (Jones, 1991; Johnson and Bates, 1996). The presence of CO has a negligible effect on measured N_2/Ar ratios, since CO concentrations in natural waters are typically 4–6 orders of magnitude lower than N_2 concentrations (Conrad and Seiler, 1980; Jones, 1991).

Standards of known O_2/N_2/Ar ratios were used to determine chemical slope corrections caused by differences in ionization efficiencies when the sample and standard have different O_2 pressures (Emerson et al., 1999; Hamme and Emerson, 2004a). Samples from April through June 2008 were analyzed at the University of Washington on a Finnigan Delta-XL IRMS, and samples from July 2008 through April 2009 were analyzed at the University of Victoria on a Finnigan MAT 253 IRMS. Systematic offsets between the two labs of about 0.1% for N_2/Ar ratios and 0.05–0.10‰ for δ^{15}N-N_2 were observed between duplicate samples from another study site. These offsets may result from uncertainties in the ionization efficiency corrections for the two instruments, but are small relative to the signals measured in Saanich Inlet.

Oxygen concentrations were determined by Carpenter-Winkler titration (Carpenter, 1965; Emerson et al., 1999), and the measured concentrations were within 6 μmol kg^{-1} (7%) of the CTD profile data, on average, between the base of the euphotic zone and the anoxic zone boundary. Sulfide was smelled in water samples from the deep basin during several cruises. However, because we did not perform measurements to determine which depths were sulfidic versus merely low-O_2, we choose to use the term anoxic broadly to refer to any waters where the CTD measured O_2 concentrations less than 10 μmol kg^{-1}. By this definition, anoxic depths include zones of NO_3^- and/or SO_4^{2-} reduction.

2.3. Ancillary data

Density measurements were obtained from two CTDs on the VENUS (Victoria Experimental Network Under the Sea) cabled observatory. The VENUS instrument platform in Saanich Inlet is located east of our sampling

station at 97 m depth, slightly deeper than the sill at 75 m, while the Strait of Georgia node is located 82 km north of our sampling station at 170 m depth (Fig. 1). Sinking particulate material and resuspended sediments occasionally clog the salinity sensor. Resulting spikes in the raw density data that were more than two standard deviations from the detrended running mean were removed, twice, and then the data were smoothed to a frequency of 6 hours. Tidal current speed predictions for Active Pass were obtained from the XTide database (http://www.flaterco.com/xtide; Pawlowicz et al., 2002), and the absolute value of the current speed was smoothed to a frequency of 25 hours.

3. Results and discussion

3.1. Subsurface respiration and renewal

Our profiles demonstrated that multiple bottom-water renewal events occurred in fall and that deep-water renewal (well below sill depth, but not renewing the bottom) occurred in spring. Renewals were characterized by increases in both O_2 concentration and density in the basin. Between our April and May 2008 cruises, deep-water renewal resulted in O_2 concentration increases of up to 100 μmol kg^{-1} between 90 and 160 m depth, but did not reach the bottom (Fig. 2). Over summer, the salinity and temperature of the bottom waters progressively decreased along a mixing line with shallower waters (Fig. 3), and the depth of the anoxic zone boundary did not deepen, both indicating that no renewal occurred.

Oxygen was detected at all depths during the September cruise (Fig. 2), and the salinity and density of the deep basin increased between August and

September (Fig. 3), demonstrating that bottom-water renewal occurred between our August and September cruises. In October, the station was still oxygenated at all depths and O_2 concentrations at 130–165 m had increased (Fig. 2). Between September and October, we expect that bottom-water O_2 concentrations would have been reduced by aerobic respiration, so the observed increase in O_2 concentration must have been caused by another renewal event. Also, salinity and density again increased in the bottom waters between September and October (Fig. 3). Together, these data indicate that at least two bottom-water renewal events occurred between our August and October cruises, repeatedly replenishing the basin with saline, oxygenated water. We will later argue that there were three renewal events during this period.

In September and October, the minimum O_2 concentration (10–15 μmol kg^{-1}) was at 120 m, while depths near the basin floor had O_2 concentrations 20 μmol kg^{-1} greater (Fig. 2). This mid-depth O_2 minimum likely resulted from deep, anoxic water being displaced upward by denser water during renewal events and mixing with oxygenated waters above and below. Similarly, Richards (1965) observed an intermediate sulfidic zone between oxygenated deep and shallow waters in September 1962 following a bottom-water renewal event in Saanich Inlet.

By December 7, bottom water O_2 had been completely consumed, and the basin remained anoxic below 125 m through at least April 2009 (Fig. 2). During winter, depths between 50 and 125 m became colder and O_2 concentrations increased as much as 100 μmol kg^{-1}. These changes likely resulted from lateral exchange of water between Saanich Inlet and surrounding waters

that was not sufficiently dense to displace the deep waters. An intermediate density, cold, ventilated water mass has been observed during winter in adjacent Haro Strait and the Strait of Georgia (LeBlond et al., 1991; Pawlowicz et al., 2007b). In April 2009, bottom waters at our station were colder and denser than the previous April (Fig. 3). Interannual variability in the density of deep waters in Saanich Inlet occurs because the proportion of the basin renewed and the properties the water masses that cause renewal also vary (Anderson and Devol, 1973; Stucchi and Giovando, 1984; Masson, 2002).

3.2. Timing and causes of renewal events

The near-yearly phenomenon of bottom-water renewal events during fall in Saanich Inlet has been previously documented, but the timing was poorly resolved and a mechanism for this inlet has not been explicitly described (Richards, 1965; Anderson and Devol, 1973; Gargett et al., 2003). We believe this is the first study to observe deep-water replacement in spring. Our monthly profiles document at least two bottom-water renewal events in fall 2008. The near-continuous measurements from the VENUS cabled observatory record the timing of these renewals and suggest that three events occurred in fall 2008. The timing of these renewal events in Saanich Inlet appears to be controlled by tidal mixing strength and the density of water outside the sill, similar to renewal processes occurring in silled regions of the Strait of Georgia. By developing an explicit mechanism for renewal in Saanich Inlet, we hope to aid researchers in predicting future events for targeted observation.

Our CTD profiles indicate that a deep-water renewal event occurred at 90–160 m between our April and May 2008 cruises (Fig. 3a). Beginning in

late April, the VENUS Saanich Inlet node at 97 m depth recorded a stepwise density increase of 0.12 kg m^{-3} d^{-1} over eight days (Fig. 4a), which must be caused by the arrival of denser waters in the basin. In this case, water at the depth of the VENUS node was renewed, resulting in the largest total density increase observed at the node for any of the renewals.

Our profile measurements show that water at the bottom of Saanich Inlet was renewed between our early August and late September cruises (Fig. 3a). Between August 9 and 18, the VENUS Saanich Inlet node detected a density increase of 0.05 kg m^{-3}, although unfortunately there is a gap in the VENUS data during the start of this event. In mid-September, this node again recorded a continuous increase in density of 0.07 kg m^{-3} over eight days. The two stepwise density increases at the VENUS node strongly suggest that two renewals occurred in the period between our early August and late September cruises. Both of these renewal events generated a smaller density change at the VENUS node than the spring renewal, likely because water primarily deeper than the 97-m node was renewed, only resulting in a density increase at the node as former bottom water was displaced upward and laterally by the renewal water.

Our CTD profiles indicate that a final renewal occurred between our late September and late October cruises (Fig. 2 and 3b). However, the VENUS node in Saanich Inlet recorded no significant density change during this period, likely indicating that this event had a minor impact on waters at 97 m depth. A VENUS node at 170 m in the Strait of Georgia (Fig. 1) measured transient potential density increases above 1024 kg m^{-3} during all the periods we identified as renewal events in Saanich Inlet (Fig. 4). We hypoth-

esize that these density increases in the Strait of Georgia demonstrate the presence of denser water in the region that could cause a renewal in Saanich Inlet (Masson, 2002). Oxygen measurements at the VENUS Saanich Inlet node were generally not helpful in determining the timing of renewal events, because some renewals resulted in O_2 increases and some in O_2 decreases, depending on how much new water at the sensor arrived from deeper, less oxygenated depths.

Each renewal event in our time series occurred during or immediately following periods of the weakest tidal currents (Fig. 4c). For our analysis, we present the absolute value of tidal current speed predictions for Active Pass, averaged with a 25-hour filter to highlight fortnightly variability. Active Pass is the nearest tidal current station to Saanich Inlet, and other locations yield similar results. Nearby observations in Puget Sound and the Strait of Georgia have shown that bottom-water flow over sills occurs during periods of weak tidal currents (Geyer and Cannon, 1982; Griffin and LeBlond, 1990). At these times, dense water can pass across the long, shallow sills in this region with minimal mixing with the fresher waters above, and retain its high density as it travels toward and into Saanich Inlet. LeBlond et al. (1991) noted that renewal events in the Strait of Georgia were specifically correlated with the weakest tidal currents that occurred at approximately monthly intervals. These authors hypothesized that the density of water masses that renew this strait can only be preserved when tidal current speeds (and therefore tidally-induced mixing rates) are below a threshold value. Similarly, our observations indicate that renewal in Saanich Inlet occurs only during the weaker of the two minima per month in average tidal current speed. A

complication in predicting the timing of renewal events in Saanich Inlet is that regional tidal currents are dominated by semi-diurnal tides, while tidal heights are dominated by diurnal tides. These tidal components do not have the same spring-neap cycle. We specifically suggest that the strength of tidal currents, rather than tidal height, be used to predict future renewal events.

Although density spikes were observed throughout the summer at the Strait of Georgia VENUS node, we only observed renewal in Saanich Inlet during spring and fall. The ultimate source of dense water to the region is upwelling along the west coast of Washington state and Vancouver Island (Masson, 2002, 2006), which lasts on average from April through October (Fig. 4d). However, the Fraser River, which generates over 50% of the freshwater discharge to the region, also has its maximum outflow in summer, when snow melt peaks (Griffin and LeBlond, 1990, Fig. 4d). The overall density of water from upwelling zones flowing through the Strait of Georgia and Haro Strait can be reduced by mixing with surface freshwater (Cannon et al., 1990; Masson, 2002; Leonov and Kawase, 2009), thereby preventing renewal in Saanich Inlet. We hypothesize that deep- and bottom-water renewal events in Saanich Inlet can only occur during spring and fall when the combination of higher upwelling at the coast and lower regional freshwater input creates the densest water just outside the inlet. The increase in bottom water density in fall likely also contributes to preventing further renewals in late fall (Fig. 3 and 4a).

3.3. Vertical diffusion rates

To determine the rate of N_2 production within the anoxic zone, we needed to quantify the rate of vertical diffusion of N_2 out of the anoxic zone. In

summer between renewal events, temperature and salinity below about 145 m steadily decreased along a linear mixing line with waters above (Fig. 3). These deep changes in salinity and temperature must be due to vertical diffusion because renewal would have increased the density, and as we will show, because along-isopycnal fluxes are small.

We used the time series of decreasing bottom water salinity and the salinity depth gradient (Fig. 5b) to determine a vertical eddy diffusion coefficient, K_z:

$$\int_{bottom\,depth}^{depth\,of\,calc.} \frac{\partial S}{\partial t} \partial z = K_z \frac{\partial S}{\partial z}\bigg|_{depth\,of\,calc.} \tag{1}$$

shown schematically in Fig. 5a. The left side of the equation is the integrated change in salinity from the depth of the calculation to the bottom of the station (190 m). Because CTD data is not available to the seafloor, we assumed that the salinity at unmeasured deeper depths was equal to the salinity at the deepest CTD depth in May, June and August (Fig. 5b). In July, the deepest CTD depth was only 176 m, so for deeper depths, we estimated the salinity as the average of the value in June and August. The term on the far right of equation 1 is the salinity depth gradient at the depth of the calculation, which we estimated from salinity data smoothed with a 10-m running mean and averaged between bracketing cruises. This calculation for K_z can be performed at every depth and for each pair of consecutive summer cruises. Values of K_z calculated for the three time periods were similar from 145 to 180 m, showing some increase with depth (Fig. 5c). Above about 130–145 m, salinity and temperature mass balances are affected by advection of a warmer, more saline water mass, which violates our assumption of a one-dimensional mass balance, so K_z values calculated for depths above 145

m are not valid. We concluded that this water mass did not penetrate below 145 m because both temperature and salinity in the deep water decreased between May and August (Fig. 3 and 5b).

In order to estimate the diffusive flux of N_2 from the anoxic zone, we calculated K_z from the top of the N_2/Ar maximum (165 m; Fig. 6) to the depth where the mass balance became inaccurate (145 m). The diffusion coefficient derived from salinity for this depth range was $(5.2 \pm 0.7) \times 10^{-5}$ m^2 s^{-1}, with the uncertainty calculated as the standard deviation of the diffusion coefficients for all months and depths (Fig. 5c). Calculating K_z from temperature or density data yielded results within 3% of the mean value from salinity. Our K_z value is higher than the value of 1×10^{-5} m^2 s^{-1} typically measured in the deep ocean (Gregg, 1989; Polzin et al., 1997), which is reasonable given the shallower depth of Saanich Inlet and the potential for enhanced mixing at the basin walls and sill. Our value is somewhat lower than eddy diffusivities of 11×10^{-5} to as much as 99×10^{-5} m^2 s^{-1} estimated for silled basins in the California borderlands when contact with basin boundaries occurs (Berelson et al., 1982; Berelson, 1991; Ledwell and Hickey, 1995; Ho et al., 2008). Although Saanich Inlet is a relatively small, steep basin, its weak tides and unusually low winds may make it more sheltered than the California borderland basins (Gargett et al., 2003).

To determine the potential effects of along-isopycnal mixing in the basin on our mass balance, we collected a profile at our station and one 12 km to the south in May, following the deep-water renewal. The along-isopycnal salinity difference between the two stations averaged 0.005, with the southern station less saline. This difference is an order of magnitude smaller than

the salinity change we measured in the deep waters of our main sampling station between May and August (0.05). If salinity had laterally homogenized between May and August such that the salinity at our sampling station decreased by 0.0025, K_z would be overestimated by 5% (0.3 m^2 s^{-1}). To account for this possible isopycnal process, we modified our error estimate for K_z to $(5.2 \pm 1.0) \times 10^{-5}$ m^2 s^{-1}.

3.4. Fixed N loss

3.4.1. Seasonal N_2/Ar cycle

We used a time series of dissolved N_2/Ar ratio measurements to quantify the rate and extent of fixed N consumption over an annual cycle. Normalizing by Ar removes much of the effect of physical processes and provides an estimate of the biologically-generated N_2 supersaturation. We present the N_2/Ar ratios in terms of their deviation from solubility equilibrium:

$$\Delta N_2/Ar = \left(\frac{(N_2/Ar)_{meas}}{(N_2/Ar)_{eq}} - 1 \right), \tag{2}$$

where $(N_2/Ar)_{meas}$ is the measured N_2/Ar ratio, $(N_2/Ar)_{eq}$ is the ratio at equilibrium with the atmosphere (Hamme and Emerson, 2004a), and $\Delta N_2/Ar$ is normally expressed in percent.

The spring 2008 deep-water renewal increased O_2 concentrations between 90 and 160 m and simultaneously decreased ΔN_2/Ar at these depths, because new water entering the inlet had lower ΔN_2/Ar (Fig. 6a–b). Over summer, the ΔN_2/Ar profiles were remarkably stable. However, as we will show, measurable rates of N_2 production are required to balance the upward diffusion of N_2 from the anoxic zone. Surface values of ΔN_2/Ar were negative in spring and summer because of surface heating, which causes Ar to become slightly

more supersaturated than N_2. The fall bottom-water renewals decreased $\Delta N_2/Ar$ by bringing in water that had lower $\Delta N_2/Ar$, but presumably significant concentrations of NO_3^- (Anderson and Devol, 1973). As the basin regained anoxia, $\Delta N_2/Ar$ increased, indicating that the rate of N_2 production exceeded its rate of removal from the deep waters by mixing. In the anoxic zone, $\Delta N_2/Ar$ was greater than 5% during six of our cruises, the highest values of $\Delta N_2/Ar$ reported in marine oxygen deficient zones to date (Table 1).

3.4.2. N_2 excess and production rates

We combined our N_2/Ar data within Saanich Inlet with measurements outside the inlet to quantify the biologically-generated N_2 excess in each month (Fig. 6c–d). Haro Strait, through which bottom water must pass to renew Saanich Inlet but where water-column fixed N loss does not occur, was used to correct for non-equilibrium effects on $\Delta N_2/Ar$ from outside the inlet, such as temperature change, bubble processes, and external fixed N loss. The average value of $\Delta N_2/Ar$ in Haro Strait was 0.50 ± 0.10 % from 2–315 m, with no depth trend (Fig. 6a–b). This mean background value of $\Delta N_2/Ar$ was subtracted from our measured values of $\Delta N_2/Ar$ to yield the N_2 excess generated within Saanich Inlet (Fig. 6c–d):

$$[N_2]_{excess} = ((\Delta N_2/Ar)_{meas} - (\Delta N_2/Ar)_{bkg}) \times [N_2]_{eq}. \quad (3)$$

Here, $\Delta N_2/Ar_{meas}$ and $\Delta N_2/Ar_{bkg}$ are the measured (Saanich Inlet) and background (Haro Strait) values, $[N_2]_{eq}$ is the N_2 concentration at equilibrium for the potential temperature and salinity of the water mass on each sampling depth and date, and $[N_2]_{excess}$ is the biological excess concentration generated

within Saanich Inlet, from water column production and benthic production that has diffused into the water column.

During a renewal event, water originally in Haro Strait mixes with water of somewhat lower density as it travels into Saanich Inlet. Mixing between water masses of different densities can generate dissolved gas supersaturations because gas solubility is a nonlinear function of temperature and salinity (Henning et al., 2006; Ito et al., 2007). However, mixing effects on the N_2 excess in Saanich Inlet are negligible because the density differences during renewals are small, and the ratio with Ar removes much of this effect. Although diffusion caused salinity and temperature in the deep basin to change between renewal events, the resultant changes in the N_2 equilibrium concentration are very small relative to the changes in $\Delta N_2/Ar$ and have a negligible effect on the estimated N_2 excess. We excluded the surface data from our estimates of the N_2 excess because the calculation is skewed by local physically-induced differential heating effects on Ar and N_2.

We calculated the vertical N_2 flux from the gradient in N_2 excess at the upper boundary of the N_2 excess maximum (Fig. 6c–d):

$$[N_2]_{flux} = K_z \frac{\partial [N_2]_{excess}}{\partial z} \rho, \tag{4}$$

where ρ is the seawater density. We calculated the mixing flux for the period between each pair of cruises, except when renewal events occurred.

Over summer, the N_2 excess profiles were very stable, and we determined the N_2 flux from the mean monthly N_2 excess gradient from 140–165 m in May through August and the mean summer K_z value. The upward N_2 flux required a mean N_2 production rate (water column plus benthic signals diffused into the water column) of 1.7 $\pm$ 0.3 mmol N_2 m^{-2} d^{-1} (Table 2).

If no N_2 production had occurred between May and August, the N_2 excess from 165–190 m would have decreased by $\sim$6 μmol kg^{-1} due to vertical mixing, which would have been easily detectable within the precision of our measurements.

From the decrease in N_2 excess between August and October, we estimate that approximately 45% of the water below 130 m was renewed at our station, which compares well with the estimates by Anderson and Devol (1973) that 64 $\pm$ 9% and 33 $\pm$ 5% of the water below 150 m was renewed during fall 1962 and 1969, respectively. If the water mass renewing the basin contained a NO_3^- concentration of $\sim$32 μmol kg^{-1} (Anderson and Devol, 1973; Masson, 2006), we would expect the mean NO_3^- concentration below 130 m to be $\sim$14 μmol kg^{-1} following the fall renewals. Complete denitrification could generate 7 μmol kg^{-1} N_2 from this NO_3^-, with additional N_2 production from the denitrified organic N of 1–2 μmol kg^{-1} N_2, depending on the process responsible and the C:N ratio of the organic matter (Froelich et al., 1979; Van Mooy et al., 2002; Dalsgaard et al., 2003). Aerobic respiration following renewal would have provided an additional fixed N input to the basin for subsequent N_2 production. We conclude that most of the N_2 production over winter was likely fueled by fixed N input during the renewal events, even though there is uncertainty in our estimate of NO_3^- concentrations after the renewals.

After the bottom-water renewals, we estimated the N_2 production rate as the sum of the rate required to generate the measured concentration increase and the rate required to balance vertical diffusion (Table 2). To calculate the increase in N_2 excess, we interpolated the N_2 excess profiles to a sampling

frequency of 1 m and then integrated the increase in N_2 excess between each cruise at each depth below the anoxic boundary. For depths below 183 m, N_2 excess measurements were not available, and we assumed that the N_2 excess was equal to the value at the deepest data point. The N_2 excess gradient was calculated from the slope of the two data points above the anoxic boundary in each month (Fig. 2 and 6c–d). For example, in February, the anoxic zone boundary was at 113 m, and we calculated the integrated increase in N_2 excess from 113–190 m, and determined the gradient in N_2 excess from measurements at 90 and 110 m. An uncertainty of 40% in the integrated N_2 excess increase for each month was calculated from the interpolated data based on the extreme assumptions that either the concentrations between measured depths were equal to the data point above or to the data point below. We applied the summer K_z estimated from 145–165 m throughout the time series, as it could not be quantified from the salinity profiles in other months. In winter, the anoxic zone boundary was shallower, and K_z at this boundary may have been greater than the summer value, due to enhanced influence from turbulence generated by the sill.

The N_2 production rates in winter were up to five times the summer rate, likely due to the flushing of the deep basin with nitrate-rich water (Anderson and Devol, 1973). The mean rate from October to December was 5.7 $\pm$ 1.7 mmol N_2 m^{-2} d^{-1} (Table 2). We expect that the rate of water column N_2 production was zero in October, when all depths were oxygenated, and higher than the mean calculated for October to December after the basin regained anoxia. The highest rate of the time series (8.1 $\pm$ 2.8 mmol N_2 m^{-2} d^{-1}) occurred from December to February, when the basin was continuously

anoxic, suggesting that a substantial supply of fixed N from the renewal events and organic matter remineralization within Saanich Inlet was available during this period. Despite no measurable increase in the N_2 excess in the summer, the N_2 production rate at this time was 20–40% of the rates over winter, indicating that fixed N supply from the spring renewal and/or vertical transport from the upper water column supported significant N_2 production rates in the summer.

To compare our rate measurements to incubation experiments in other environments, we estimated the N_2 production rate per volume, assuming a constant rate below the anoxic boundary for each pair of cruises (Fig. 2). This estimate provides a lower bound for the production rates, as the denitrifying zone may have been narrower. The volume-normalized N_2 production rates in Saanich Inlet are higher than those measured in the Black Sea and Arabian Sea from ^{15}N incubation experiments, resulting in the highest values of $\Delta N_2/Ar$ measured to date, despite frequent flushing of oxygenated, low-N_2 water into the basin (Table 1).

3.4.3. $\delta^{15}N$-N_2 of gross and excess N_2

The maximum value of $\delta^{15}N$-N_2 coincided with the maximum N_2 excess in spring and summer, indicating that fixed N consumption must have approached or gone to completion (Fig. 7). The ^{15}N isotope effect on NO_3^- associated with incomplete marine denitrification is ∼20–30‰ (Brandes et al., 1998; Barford et al., 1999; Granger et al., 2008), whereas complete denitrification has a negligible isotope effect because the entire reactant fixed N pool is converted to N_2 (Brandes and Devol, 2002; Sigman et al., 2003; Deutsch et al., 2004). Complete fixed N consumption via anammox should similarly

produce a negligible isotope effect.

We determined the isotopic composition of the excess N_2 by a mass balance incorporating the background profile measurements (Fuchsman et al., 2008):

$$R_{meas}\left(\Delta\frac{N_2}{Ar}meas\ +\ 1\right)[N_2]_{eq} = R_{bkg}\left(\Delta\frac{N_2}{Ar}bkg\ +\ 1\right)[N_2]_{eq} + R_{excess}[N_2]_{excess} \tag{5}$$

where R is the ratio of ^{15}N-N_2/^{14}N-N_2. For the background isotopic composition of N_2, we used the mean value of 0.73 ± 0.03‰ measured in Haro Strait (Fig. 7a).

In the deep basin, the average isotopic composition of the N_2 excess in spring and summer 2008 was 7.5 ± 1.2‰ (Fig. 8). Some of the spread in values may result from the samples from April through June being run in a different lab than the July and August profiles. The values of δ^{15}N of the N_2 excess compare well with previous measurements of δ^{15}N-NO_3^- in Saanich Inlet averaging 7.5‰ in February and May 2004 (E. Galbraith, personal communication). In addition, Nakatsuka et al. (1992) performed a mesocosm experiment in Saanich Inlet and determined that the isotopic composition of particulate organic N exported from the euphotic zone averaged 7‰. These results suggest that the isotopic composition of the biologically-produced N_2 was similar to the original isotopic composition of the fixed N pool, supporting our conclusion that fixed N consumption approached completion in spring and summer. During the bottom water renewal, δ^{15}N-N_2 of the N_2 excess and ΔN_2/Ar both decreased. Following the renewal, they increased again, suggesting a shift from incomplete fixed N consumption (when the anoxic zone was newly reestablished) toward complete consumption (in spring). A

shift in the isotopic composition of the fixed N source, from organic matter respired within Saanich Inlet to nutrients advected into Saanich Inlet during the renewal, also could have played a role in altering δ^{15}N-N_2.

A sharp increase in δ^{15}N-N_2 at the surface was measured in all months when surface samples were collected (Fig. 7). Photochemical production of CO in surface waters may cause our measured values of δ^{15}N-N_2 to be biased high. However, this process would have a negligible effect on the measured N_2 isotopic composition below the euphotic zone (0–15 m). Rapid surface heating and N_2 fixation could both generate enrichments in ^{15}N-N_2, but the fractionation factors for these processes combined with the observed changes in surface temperature and ΔN_2/Ar are not sufficient to generate the measured enrichments of about 0.2‰ (Hoering and Ford, 1960; Minagawa and Wada, 1986; Knox et al., 1992).

4. Conclusions

We collected an annual time series of dissolved O_2 concentration, N_2/Ar ratios and δ^{15}N-N_2 in Saanich Inlet from April 2008 to April 2009. Four deep- or bottom-water renewal events occurred during our study and each was correlated with periods of weak tidal currents, similar to the timing of renewal in nearby waters (LeBlond et al., 1991; Masson, 2002). During periods of low tidal mixing, the density of inflowing water is retained as it crosses the sill and enters the basin. Renewal occurred in spring and fall when coastal upwelling brought dense water into the region, but the rate of freshwater discharge was not too high.

In the bottom waters, ΔN_2/Ar was greater than 5% during six of our

cruises, far higher than values reported in the Black Sea and the Arabian Sea (Table 1). We quantified the biological N_2 production rate and found very high rates on a per volume basis, likely driven by input of new NO_3^- from renewal events. In late spring and summer, the maximum in δ^{15}N-N_2 coincided with the maximum N_2 excess, indicating that denitrification/anammox approached completion in those months.

Our measurements in Saanich Inlet help to improve our understanding of the N cycle in intermittently anoxic zones. Our fixed N loss rates derived from the water column N_2 excess account for all pathways to N_2 production. Unlike incubation experiments, they provide an integrated, basin-scale rate of fixed N loss. Application of these methods in more regions will help to reduce uncertainties in the marine N budget during a period of global change.

5. Acknowledgements

We thank Ian Beveridge, Paul Covert, Courtney Dean, Karina Giesbrecht, and Victoria Gray for assistance with field work and sample processing. Alice Chang, Jay Cullen, Vera Pospelova, and Sarah Thornton shared lab space and equipment. Jody Klymak helped with our diffusivity and renewal analysis, and Richard Dewey assisted with processing and interpreting the VENUS and tidal data. Mark Altabet and two anonymous reviewers helped to improve the manuscript. We used data from the following sources in our figures and calculations: CTD data from VENUS (http://venus.uvic.ca), upwelling index data from NOAA (http://pfeg.noaa.gov), and Fraser River outflow measurements from the Water Survey of Canada (http://scitech.pyr.ec.gc.ca/waterweb). This work was supported by NSERC under 328290-2006 to Hamme, 356654-

08 and 134794-2006 to Kim Juniper, and research awards to Manning and Bourbonnais. Lab equipment was funded by grants from the CFI and BCKDF to Hamme. Additionally, Manning was supported by the Bob Wright Scholarship and the Meteorological Service of Canada.

References

Anderson, J.J., Devol, A.H., 1973. Deep water renewal in Saanich Inlet, an intermittently anoxic basin. Estuarine and Coastal Marine Science 1, 1–10.

Barford, C.C., Montoya, J.P., Altabet, M.A., Mitchell, R., 1999. Steady-state nitrogen isotope effects of N_2 and N_2O production in *Paracoccus denitrificans*. Applied and Environmental Microbiology 65, 989–994.

Bender, M.L., Tans, P.P., Ellis, J., Orchardo, J., Habfast, K., 1994. A high precision isotope ratio mass spectrometry method for measuring the O_2/N_2 ratio of air. Geochimica et Cosmochimica Acta 58, 4751–4758.

Berelson, W., Hammond, D., Fuller, C., 1982. Radon-222 as a tracer for mixing in the water column and benthic exchange in the southern California borderland. Earth and Planetary Science Letters 61, 41–54.

Berelson, W.M., 1991. The flushing of two deep-sea basins, southern California borderland. Limnology and Oceanography 36, 1150–1166.

Brandes, J.A., Devol, A.H., 2002. A global marine-fixed nitrogen isotopic budget: Implications for Holocene nitrogen cycling. Global Biogeochemical Cycles 16, 1120, doi:10.1029/2001GB001856.

Brandes, J.A., Devol, A.H., Yoshinari, T., Jayakumar, D.A., Naqvi, S.W.A., 1998. Isotopic composition of nitrate in the central Arabian Sea and eastern tropical North Pacific: A tracer for mixing and nitrogen cycles. Limnology and Oceanography 43, 1680–1689.

Cannon, G.A., Holbrook, J.R., Pashinski, D.J., 1990. Variations in the onset of bottom-water intrusions over the entrance sill of a fjord. Estuaries and Coasts 13, 31–42.

Carpenter, J.H., 1965. The Chesapeake Bay Institute technique for the Winkler dissolved oxygen method. Limnology and Oceanography 10, 141–143.

Codispoti, L.A., 2007. An oceanic fixed nitrogen sink exceeding 400 Tg N a^{-1} vs the concept of homeostasis in the fixed-nitrogen inventory. Biogeosciences 4, 233–253.

Conrad, R., Seiler, W., 1980. Photooxidative production and microbial consumption of carbon monoxide in seawater. FEMS Microbiology Letters 9, 61–64.

Dalsgaard, T., Canfield, D.E., Petersen, J., Thamdrup, B., Acuña-González, J., 2003. N_2 production by the anammox reaction in the anoxic water column of Golfo Dulce, Costa Rica. Nature 422, 606–608.

Deutsch, C., Sigman, D.M., Thunell, R.C., Meckler, A.N., Haug, G.H., 2004. Isotopic constraints on glacial/interglacial changes in the oceanic nitrogen budget. Global Biogeochemical Cycles 18, GB4012, doi:10.1029/2003GB002189.

Devol, A., 2003. Nitrogen cycle - solution to a marine mystery. Nature 422, 575–576.

Devol, A., Uhlenhopp, A., Naqvi, S., Brandes, J., Jayakumar, D., Naik, H., Gaurin, S., Codispoti, L., Yoshinari, T., 2006. Denitrification rates and excess nitrogen gas concentrations in the Arabian Sea oxygen deficient zone. Deep-Sea Research I 53, 1533–1547.

Emerson, S., Cranston, R.E., Liss, P.S., 1979. Redox species in a reducing fjord: equilibrium and kinetic considerations. Deep-Sea Research I 26, 859–878.

Emerson, S., Stump, C., Wilbur, D., Quay, P., 1999. Accurate measurement of O_2, N_2, and Ar gases in water and the solubility of N_2. Marine Chemistry 64, 337–347.

Froelich, P., Klinkhammer, G., Bender, M., Luedtke, N., Heath, G., Cullen, D., Dauphin, P., Hammond, D., Hartman, B., Maynard, V., 1979. Early oxidation of organic matter in pelagic sediments of the eastern equatorial Atlantic: suboxic diagenesis. Geochimica et Cosmochimica Acta 43, 1075–1090.

Fuchsman, C., Murray, J., Konovalov, S., 2008. Concentration and natural stable isotope profiles of nitrogen species in the Black Sea. Marine Chemistry 111, 90–105.

Gargett, A.E., Stucchi, D., Whitney, F., 2003. Physical processes associated with high primary production in Saanich Inlet, British Columbia. Estuarine, Coastal and Shelf Science 56, 1141–1156.

Geyer, W.R., Cannon, G.A., 1982. Sill processes related to deep water renewal in a fjord. Journal of Geophysical Research 87, 7985–7996.

Glazer, B.T., Luther, G.W., Konovalov, S.K., Friederich, G.E., Trouwborst, R.E., Romanov, A.S., 2006. Spatial and temporal variability of the Black Sea suboxic zone. Deep-Sea Research II 53, 1756–1768.

Granger, J., Sigman, D.M., Lehmann, M.F., Tortell, P.D., 2008. Nitrogen and oxygen isotope fractionation during dissimilatory nitrate reduction by denitrifying bacteria. Limnology and Oceanography 53, 2533–2545.

Gregg, M.C., 1989. Scaling turbulent dissipation in the thermocline. Journal of Geophysical Research 94, 9686–9698.

Griffin, D.A., LeBlond, P.H., 1990. Estuary/ocean exchange controlled by spring-neap tidal mixing. Estuarine, Coastal and Shelf Science 30, 275–297.

Groffman, P.M., Altabet, M.A., Böhlke, J.K., Butterbach-Bahl, K., David, M.B., Firestone, M.K., Giblin, A.E., Kana, T.M., Nielsen, L.P., Voytek, M.A., 2006. Methods for measuring denitrification: diverse approaches to a difficult problem. Ecological Applications 16, 2091–2122.

Gruber, N., 2004. The dynamics of the marine nitrogen cycle and its influence on atmospheric CO_2, in: Follows, M., Oguz, T. (Eds.), The Ocean Carbon Cycle and Climate. Kluwer Academic, Dordrecht, pp. 97–148.

Hamme, R., Emerson, S., 2004a. The solubility of neon, nitrogen and argon in distilled water and seawater. Deep-Sea Research I 51, 1517–1528.

Hamme, R.C., Emerson, S.R., 2004b. Measurement of dissolved neon by isotope dilution using a quadrupole mass spectrometer. Marine Chemistry 91, 53–64.

Hannig, M., Lavik, G., Kuypers, M., Woebken, D., Martens-Habbena, W., Jurgens, K., 2007. Shift from denitrification to anammox after inflow events in the central Baltic Sea. Limnology and Oceanography 52, 1336–1345.

Henning, C.C., Archer, D., Fung, I., 2006. Argon as a tracer of cross-isopycnal mixing in the thermocline. Journal of Physical Oceanography 36, 2090–2105.

Ho, D.T., Ledwell, J.R., Smethie, W.M., 2008. Use of SF_5CF_3 for ocean tracer release experiments. Geophysical Research Letters 35, L04602, doi:10.1029/2007GL032799.

Hoering, T.C., Ford, H.T., 1960. The isotope effect in the fixation of nitrogen by *Azotobacter*. Journal of the American Chemical Society 82, 376–378.

Hulth, S., Aller, R.C., Canfield, D.E., Dalsgaard, T., Engstrm, P., Gilbert, F., Sundbck, K., Thamdrup, B., 2005. Nitrogen removal in marine environments: recent findings and future research challenges. Marine Chemistry 94, 125–145.

Ito, T., Deutsch, C., Emerson, S., Hamme, R.C., 2007. Impact of diapycnal mixing on the saturation state of argon in the subtropical North Pacific. Geophysical Research Letters 34, L09602, doi:10.1029/2006GL029209.

Johnson, J.E., Bates, T.S., 1996. Sources and sinks of carbon monoxide in the mixed layer of the tropical South Pacific Ocean. Global Biogeochemical Cycles 10, 347–359.

Jones, R.D., 1991. Carbon monoxide and methane distribution and consumption in the photic zone of the Sargasso Sea. Deep-Sea Research A 38, 625–635.

Knox, M., Quay, P.D., Wilbur, D., 1992. Kinetic isotopic fractionation during air-water gas transfer of O_2, N_2, CH_4, and H_2. Journal of Geophysical Research 97, 20335–20343.

Kuypers, M.M.M., Lavik, G., Woebken, D., Schmid, M., Fuchs, B.M., Amann, R., Jørgensen, B.B., Jetten, M.S.M., 2005. Massive nitrogen loss from the Benguela upwelling system through anaerobic ammonium oxidation. Proceedings of the National Academy of Sciences of the USA 102, 6478–6483.

Kuypers, M.M.M., Sliekers, A.O., Lavik, G., Schmid, M., Jørgensen, B.B., Kuenen, J.G., Damsté, J.S.S., Strous, M., Jetten, M.S.M., 2003. Anaerobic ammonium oxidation by anammox bacteria in the Black Sea. Nature 422, 608–611.

Larsson, U., Elmgren, R., Wulff, F., 1985. Eutrophication and the Baltic Sea: Causes and consequences. Ambio 14, 9–14.

LeBlond, P., Ma, H., Doherty, F., Pond, S., 1991. Deep and intermediate water replacement in the Strait of Georgia. Atmosphere-Ocean 29, 288–312.

Ledwell, J.R., Hickey, B.M., 1995. Evidence for enhanced boundary mixing in the Santa Monica Basin. Journal of Geophysical Research 100, 20665–20680.

Leonov, D., Kawase, M., 2009. Sill dynamics and fjord deep water renewal: Idealized modeling study. Continental Shelf Research 29, 221–233.

Malakoff, D., 1998. Coastal ecology: Death by suffocation in the Gulf of Mexico. Science 281, 190–192.

Masson, D., 2002. Deep water renewal in the Strait of Georgia. Estuarine, Coastal and Shelf Science 54, 115–126.

Masson, D., 2006. Seasonal water mass analysis for the Straits of Juan de Fuca and Georgia. Atmosphere-Ocean 44, 1–15.

Minagawa, M., Wada, E., 1986. Nitrogen isotope ratios of red tide organisms in the East China Sea: A characterization of biological nitrogen fixation. Marine Chemistry 19, 245–259.

Nakatsuka, T., Handa, N., Wada, E., Wong, C.S., 1992. The dynamic changes of stable isotopic ratios of carbon and nitrogen in suspended and sedimented particulate organic matter during a phytoplankton bloom. Journal of Marine Research 50, 267–296.

Naqvi, S.W.A., Jayakumar, D.A., Narvekar, P.V., Naik, H., Sarma, V.V.S.S., D'Souza, W., Joseph, S., George, M.D., 2000. Increased marine production of N_2O due to intensifying anoxia on the Indian continental shelf. Nature 408, 346–349.

Pawlowicz, R., Baldwin, S.A., Muttray, A., Schmidtova, J., Laval, B., Lamont, G., 2007a. Physical, chemical, and microbial regimes in an anoxic fjord (Nitinat Lake). Limnology and Oceanography 52, 1002–1017.

Pawlowicz, R., Beardsley, B., Lentz, S., 2002. Classical tidal harmonic analysis including error estimates in MATLAB using T_TIDE. Computers & Geosciences 28, 929–937.

Pawlowicz, R., Riche, O., Halverson, M., 2007b. The circulation and residence time of the Strait of Georgia using a simple Mixing-Box approach. Atmosphere-Ocean 45, 173–194.

Polzin, K.L., Toole, J.M., Ledwell, J.R., Schmitt, R.W., 1997. Spatial variability of turbulent mixing in the abyssal ocean. Science 276, 93–96.

Richards, F.A., 1965. Anoxic basins and fjords, in: Riley, J.P., Skirrow, G. (Eds.), Chemical Oceanography. Academic Press, London. volume 1, pp. 611–645.

Sigman, D.M., Robinson, R., Knapp, A.N., van Geen, A., McCorkle, D.C., Brandes, J.A., Thunell, R.C., 2003. Distinguishing between water column and sedimentary denitrification in the Santa Barbara Basin using the stable isotopes of nitrate. Geochemistry, Geophysics, Geosystems 4, 1040, doi:10.1029/2002GC000384.

Smith, S., 1984. Phosphorus versus nitrogen limitation in the marine environment. Limnology and Oceanography 29, 1149–1160.

Stucchi, D.J., Giovando, L.F., 1984. Deep water renewal in Saanich Inlet,

B.C. Canadian Technical Report of Hydrography and Ocean Sciences 38, 7–15.

Thamdrup, B., Dalsgaard, T., Jensen, M., Ulloa, O., Farias, L., Escribano, R., 2006. Anaerobic ammonium oxidation in the oxygen-deficient waters off northern Chile. Limnology and Oceanography 51, 2145–2156.

Timothy, D.A., Soon, M.Y.S., 2001. Primary production and deep-water oxygen content of two British Columbian fjords. Marine Chemistry 73, 37–51.

Tunnicliffe, V., Dewey, R., Smith, D., 2003. Research plans for a mid-depth cabled seafloor observatory in western Canada. Oceanography 16, 53–59.

Tyrrell, T., 1999. The relative influences of nitrogen and phosphorus on oceanic primary production. Nature 400, 525–531.

Van Mooy, B.A.S., Keil, R.G., Devol, A.H., 2002. Impact of suboxia on sinking particulate organic carbon: Enhanced carbon flux and preferential degradation of amino acids via denitrification. Geochimica et Cosmochimica Acta 66, 457–465.

Table 1: N_2 excess and N_2 production rates in oxygen-deficient zones

Location	$\Delta N_2/Ar$ (%)	N_2 excess (μmol kg^{-1})	N_2 production rate (nmol kg^{-1} d^{-1})	Reference
Arabian Sea	2.5 – 3.5	8 – 12	9.1 ± 1.0 (open ocean)†	Devol et al. (2006)
			33.2 ± 12.4 (coastal)†	
Black Sea	1.5 – 3.0	7.5 – 20		Fuchsman et al. (2008)
			1 – 11†	Jensen et al. (2008)
Saanich Inlet	2.7 – 5.2	11 – 25	43 ± 10 to 103 ± 35‡	This study

†Determined from ^{15}N enrichment incubations

‡Determined from N_2/Ar mass balance

Table 2: Rates of N_2 production in Saanich Inlet (2008-2009)

Months	N_2 production rate to balance diffusion (mmol m^{-2} d^{-1})	N_2 production rate to generate increase (mmol m^{-2} d^{-1})	Total rate of N_2 production (mmol m^{-2} d^{-1})
May – Aug	1.7 ± 0.3	0	1.7 ± 0.3
Oct – Dec	1.5 ± 0.3	4.2 ± 1.7	5.7 ± 1.7
Dec – Feb	1.2 ± 0.2	6.9 ± 2.8	8.1 ± 2.8
Feb – Apr	1.5 ± 0.3	3.0 ± 1.2	4.5 ± 1.2

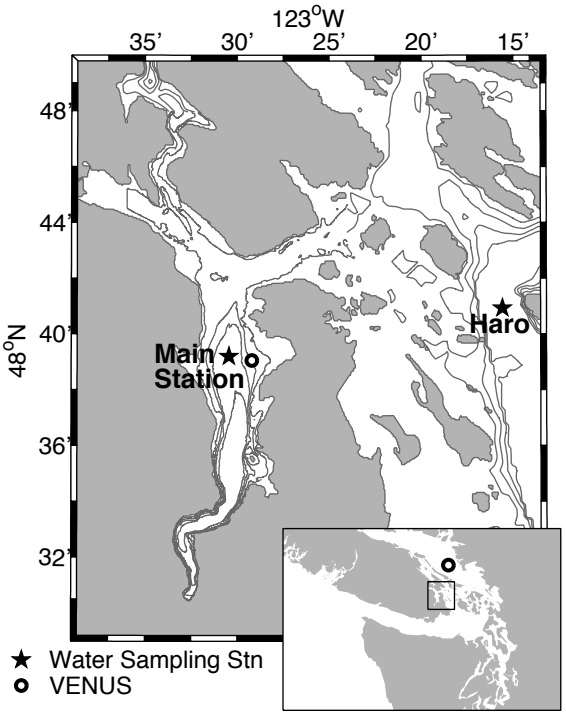

Figure 1: Bathymetric map of Saanich Inlet and surrounding waters, showing the location of the VENUS CTD, the sampling station in Saanich, and the background station in Haro Strait. Contours represent 50 m depth intervals. Inset map shows the location of the VENUS CTD in the Strait of Georgia, along with the wider region of Vancouver Island, and coastal Washington state and British Columbia.

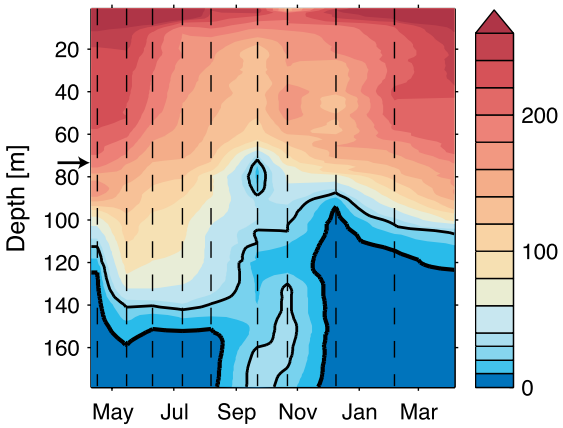

Figure 2: Contour plot of O_2 concentrations (μmol kg^{-1}) at the sampling station measured by the CTD O_2 sensor. Dashed lines indicate the timing of cruises and the arrow indicates the sill depth (75 m). Renewal events are highlighted by black contour lines corresponding to 10 μmol kg^{-1} (anoxic boundary, thick line) and 30 μmol kg^{-1} (thin line).

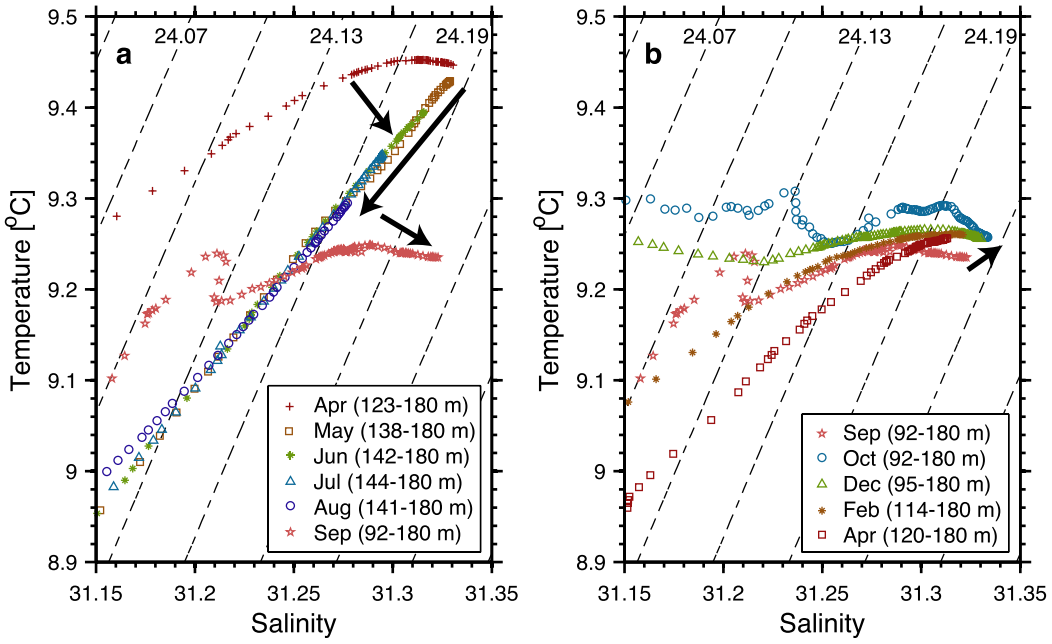

Figure 3: Temperature/salinity plot of water above 180 m in Saanich Inlet from a) April to September 2008 and b) September 2008 to April 2009. Depths in the legend refer to the range of depths plotted for each month. Dashed lines are potential density (σ_θ, kg m^{-3}). Changes generated by renewal events and vertical diffusion are indicated with arrows.

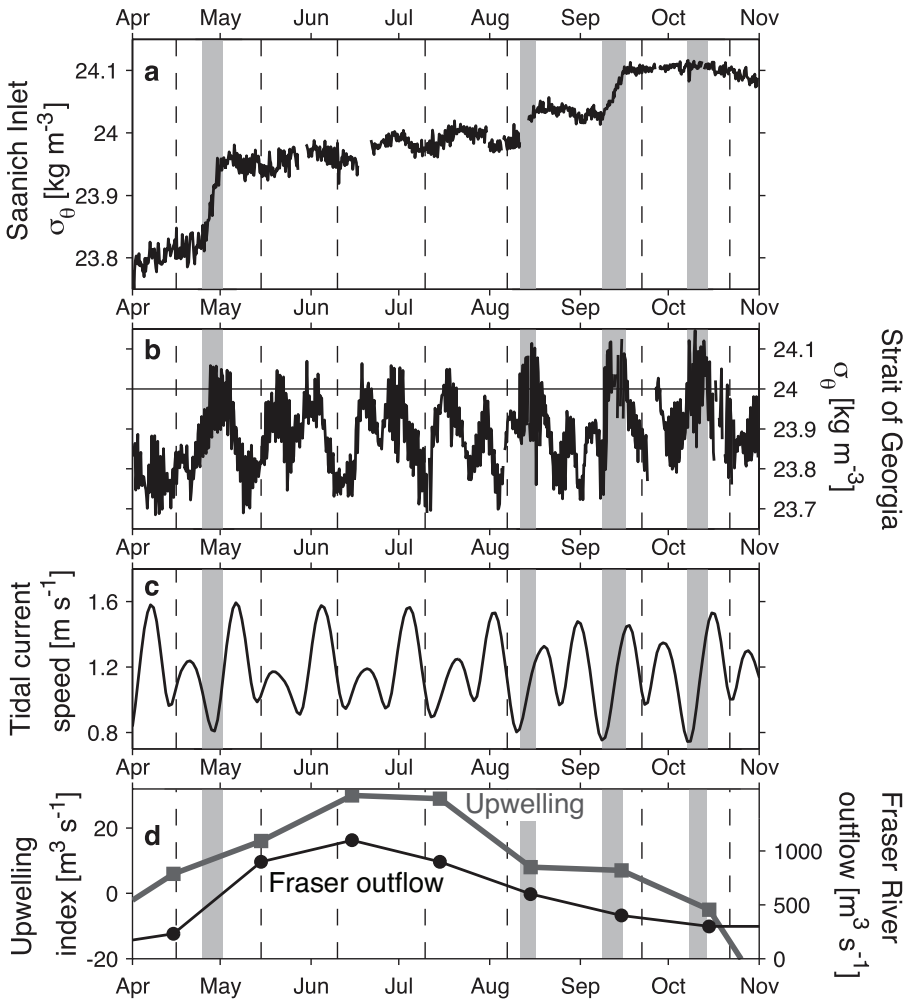

Figure 4: Potential density (σ_θ, kg m^{-3}) measured by the VENUS observatory in a) Saanich Inlet and b) the Strait of Georgia. c) Magnitude of tidal current speed (m s^{-1}) at Active Pass in the Strait of Georgia. d) Mean monthly upwelling index at 48° N, 125° W (m^3 s^{-1}, square markers) and Fraser River outflow (m^3 s^{-1}, circlular markers). Vertical dashed lines indicate timing of cruises and grey bars indicate renewal events, which were defined as periods with a continuous σ_θ increase of at least 0.004 kg m^{-3} d^{-1} for several days at the Saanich Inlet node (April–September). The October renewal timing was estimated from the period with mean daily σ_θ at the Strait of Georgia node continuously above 24 kg m^{-3} (horizontal line in panel b).

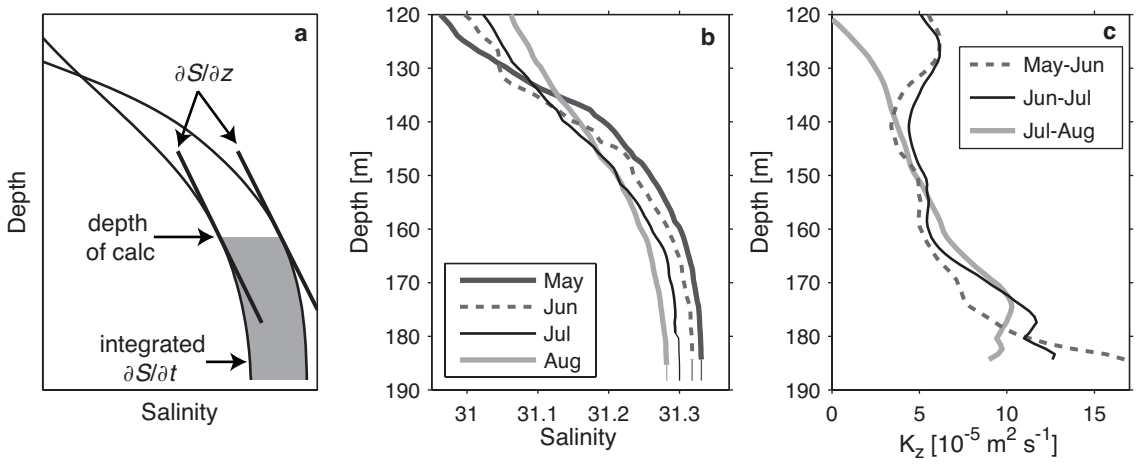

Figure 5: a) Idealized schematic representing the calculation of K_z from two salinity profiles. The grey area indicates the change in salinity between the two observation times ($\partial S/\partial t$) integrated from the depth of the calculation to the bottom of the station (left side of equation 1). The depth gradient in salinity ($\partial S/\partial z$) was evaluated at the depth of the calculation for both profiles and then averaged (far right side of equation 1). b) Observed salinity profiles in deep Saanich Inlet, May–August 2008. Thinner lines at bottom indicate extrapolation of each salinity profile to the full depth of the station. c) Depth profiles of K_z calculated from salinity data in b).

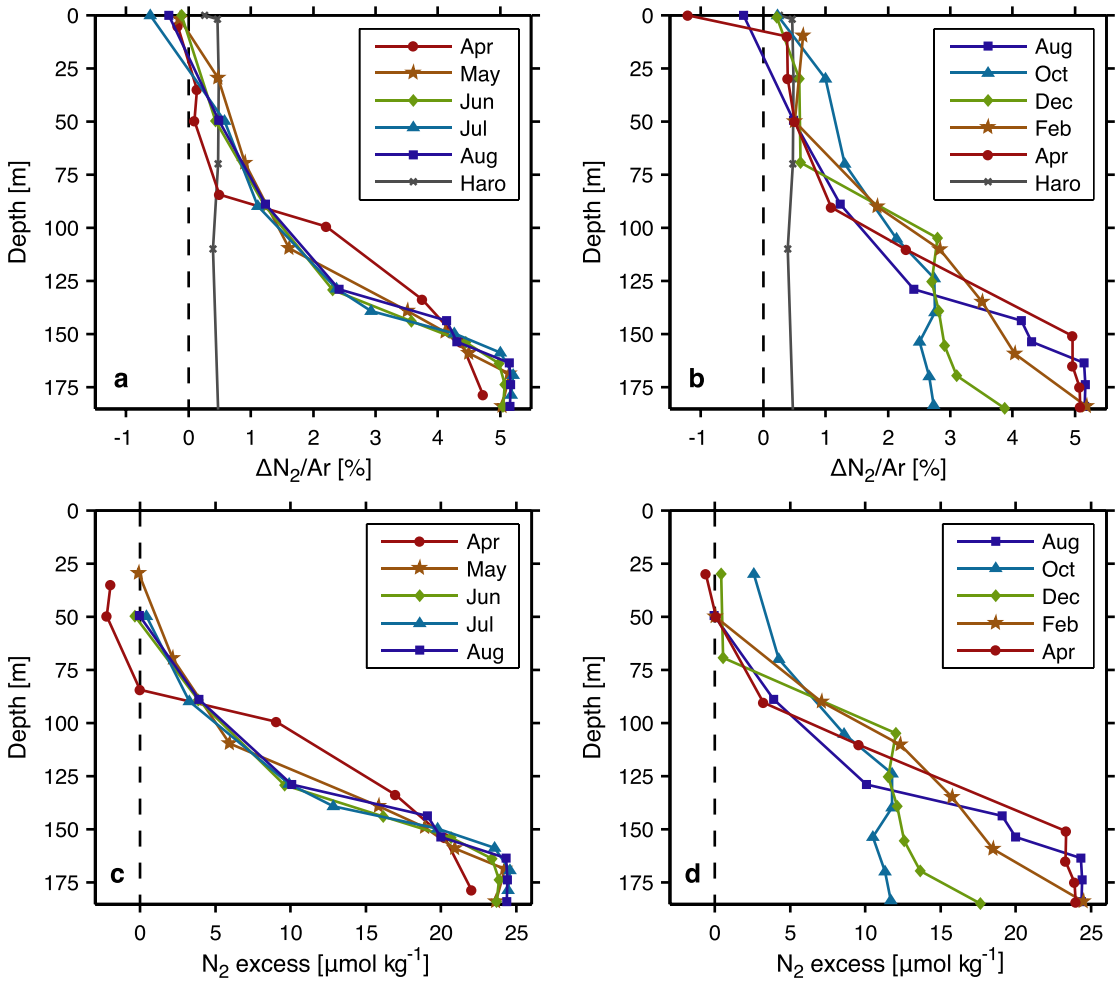

Figure 6: $\Delta N_2/Ar$ (%) from a) April to August 2008 and b) August 2008 to April 2009. The background Haro profile extended down to 315 m with very similar values. Biological N_2 excess generated within Saanich Inlet (μmol kg^{-1}) from c) April to August 2008 and d) August 2008 to April 2009. The vertical dashed line in each plot represents solubility equilibrium.

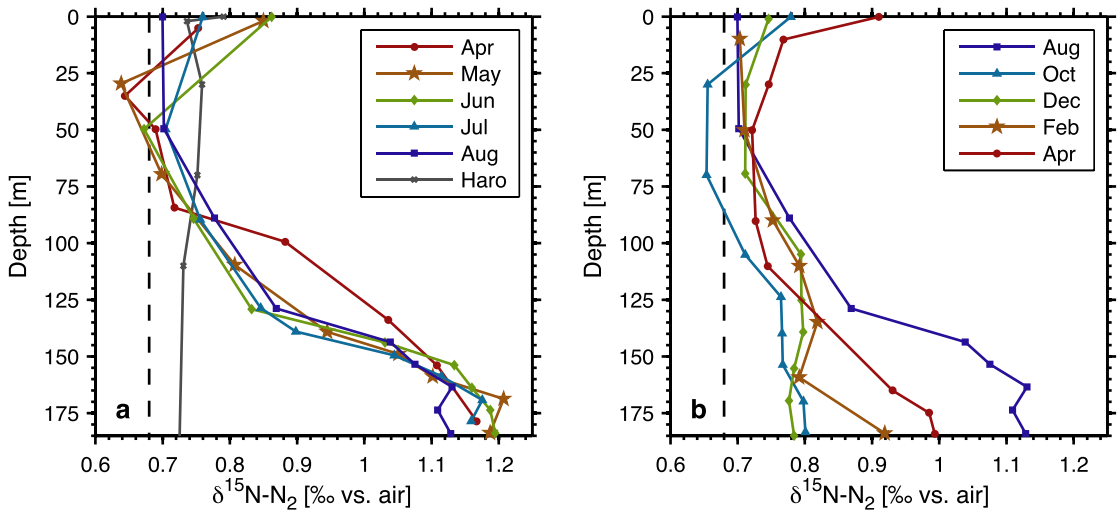

Figure 7: δ^{15}N-N_2 (‰ vs. air) from a) April to August 2008 and b) August 2008 to April 2009. Measurements in Haro Strait had stable values down to 315 m. The vertical dashed line at 0.68‰ represents equilibrium with the atmosphere (Knox et al., 1992).

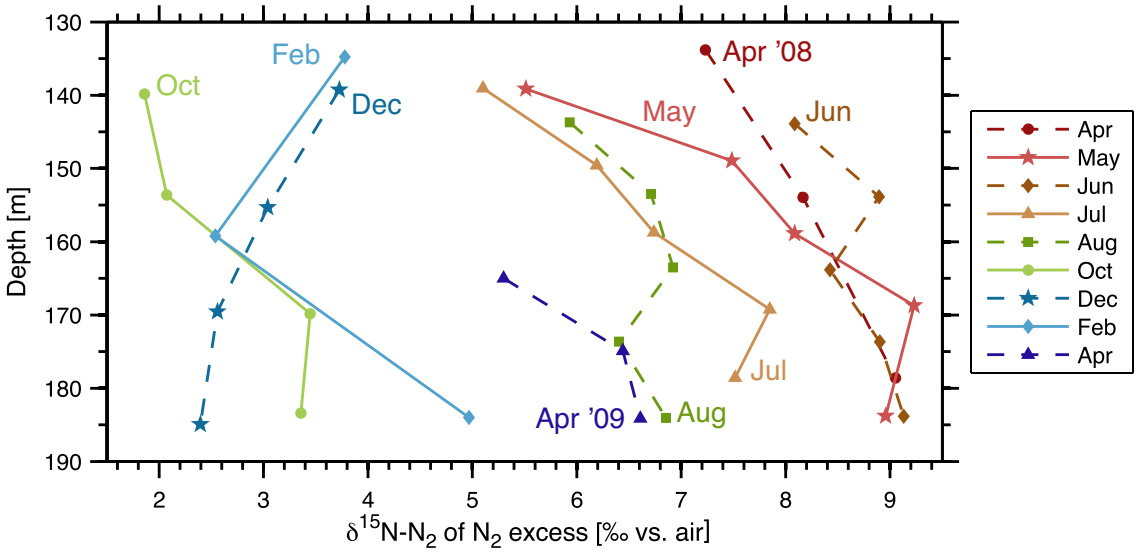

Figure 8: Isotopic composition of the N_2 excess, δ^{15}N-N_2 (‰ vs. air), in the deep basin.